NASA Contractor Report 178068

ICASE REPORT NO. 86-9

NASA-CR-178068
19860013422

ICASE

NON-REFLECTING BOUNDARY CONDITIONS FOR THE COMPRESSIBLE NAVIER-STOKES EQUATIONS

Saul Abarbanel

Alvin Bayliss

Liviu Lustman

Contract Nos. NAS1-17070 and NAS1-18107

March 1986

INSTITUTE FOR COMPUTER APPLICATIONS IN SCIENCE AND ENGINEERING
NASA Langley Research Center, Hampton, Virginia 23665

Operated by the Universities Space Research Association

National Aeronautics and
Space Administration

Langley Research Center
Hampton, Virginia 23665

NON-REFLECTING BOUNDARY CONDITIONS

FOR THE COMPRESSIBLE NAVIER-STOKES EQUATIONS

Saul Abarbanel
Tel-Aviv University

Alvin Bayliss
Exxon Corporate Research Science Laboratories

Liviu Lustman
Institute for Computer Applications in Science and Engineering

Abstract

A small perturbation analysis, in the long wavelength regime, is used to obtain the downstream boundary condition for the pressure for the flow over a flat plate. The methodology is extendable to other geometries. Numerical results for high Reynolds number laminar flows show great improvement in convergence rate to steady state as well as in the quality of the results.

This work was supported in part by the Air Force Office of Scientific Research (NAN), AFSC, United States Air Force under Grant AFOSR-82-0136E while the first author was at M.I.T.; and in part by NASA Contracts No. NAS1-17070 and NAS1-18107 while the authors were in residence at ICASE, NASA Langley Research Center, Hampton, VA 23665-5225.

1. INTRODUCTION

Since the early 1970's there has been growing attention paid to the numerical solution of the full time-dependent, viscous, compressible Navier-Stokes equations of fluid mechanics; see inter-alia [1], [4]. A vexing and still open issue is the formulation of "downstream" or "outflow" boundary conditions. One common strategy for flows evolving to steady state has been to assume that the particular geometry considered allows the imposition of the infinity-downstream steady state conditions at the relevant boundary of the computational domain. For example, for flow in a pipe, the downstream condition might be taken from the fully-developed, steady-state parabolic profile. For a semi-infinite flat plate at zero angle of attack, it is usually assumed that "sufficiently far" downstream, the free stream conditions predicted by boundary layer theory are sufficient for stating the corresponding boundary conditions.

Numerical experiments (see e.g., [5-6]) with time-consistent codes have shown that taking $p = p_\infty$ for the downstream boundary conditions leads to very slow convergence to steady state. This phenomenon is aggravated with increased Reynolds numbers, because the spatial resolution of the boundary layer then leads, via the von Neumann stability analysis, to very small time steps. It can be seen from the results of Rudy and Strikwerda [5] that the retardation of the convergence to steady state is caused mainly by the slow decay of relatively long wavelength disturbances. They tried to account for this by proposing a boundary condition on the pressure of the form

$$\frac{\partial p}{\partial t} - \rho c \frac{\partial u}{\partial t} + \alpha(p - p_\infty) = 0 \qquad (1.1)$$

where ρ is the density, $c = (\gamma p/\rho)^{1/2}$ is the speed of sound, and α is a free parameter which is "tuned" so as to optimize the convergence rate to steady state. Note, that in any case at steady state, the downstream boundary pressure has the free-stream value. Their treatment greatly accelerated the convergence rate; its derivation, however, is basically "hyperbolic."

In this paper we propose to derive downstream boundary conditions using a different methodology. The basic idea is to perturb the Navier-Stokes equations around some approximation (usually a fairly crude one) to the steady state solution in the downstream region. The linearized partial differential equations for the perturbed quantities are then attacked using a modal form for their solution. The resulting ordinary differential equations present an eigenvalue problem which is solved assuming very long wavelengths. This eigenvalue problem yields the decay rate for long waves and their phase velocity. With these two quantities, as functions of the Mach number and the Reynolds number, one can use the modal form of the perturbed solution to obtain the desired boundary condition.

In section 2 we give the derivation of the eigenvalue problem and the boundary condition for the particular case of the flow past a two-dimensional flat plate.

Numerical results are presented in section 3 for the case of subsonic Mach number, $M_\infty = 0.4$. The corresponding Reynolds numbers per foot is 3×10^5. The numerical experiments are carried out for semi-infinite plates with the outflow boundary taken at various locations downstream of the leading edge.

2. THEORETICAL DEVELOPMENT

The geometry under consideration is shown in the sketch below.

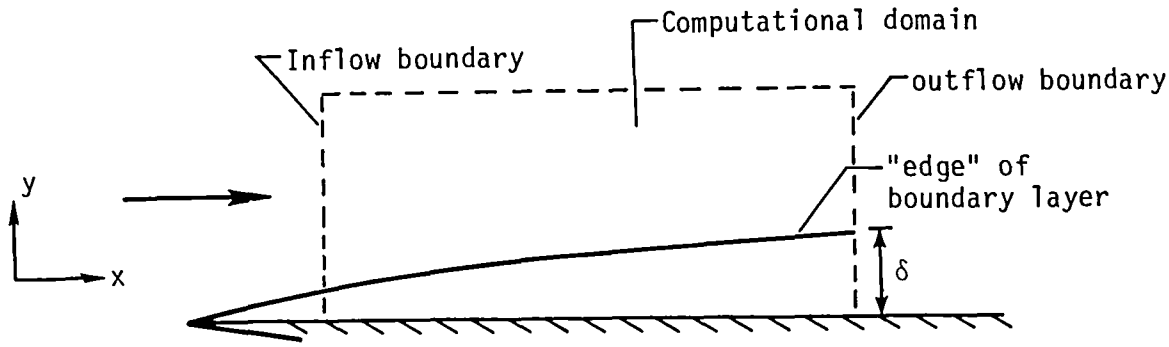

The two-dimensional compressible Navier-Stokes equations governing the flow may be written in conservation form as

$$\frac{\partial \overline{U}}{\partial t} + \frac{\partial \overline{F}}{\partial x} + \frac{\partial \overline{G}}{\partial y} = 0 \tag{2.1}$$

where

$$\overline{U} = \begin{bmatrix} \rho \\ \rho u \\ \rho v \\ E \end{bmatrix}, \qquad \overline{F} = \begin{bmatrix} \rho u \\ \rho u^2 + \tau_{xx} \\ \rho uv + \tau_{yx} \\ (E + \tau_{xx})u + \tau_{yx} v - k \frac{\partial T}{\partial x} \end{bmatrix} \tag{2.2}$$

$$G = \begin{bmatrix} \rho u \\ \rho uv + \tau_{xy} \\ \rho v^2 + \tau_{yy} \\ (E + \tau_{yy})v + \tau_{xy} u - k \frac{\partial T}{\partial y} \end{bmatrix}.$$

and

$$\tau_{xx} = p - 2\mu \frac{\partial u}{\partial x} - \lambda\left(\frac{\partial u}{\partial x} + \frac{\partial v}{\partial y}\right)$$

$$\tau_{yy} = p - 2\mu \frac{\partial v}{\partial y} - \lambda\left(\frac{\partial u}{\partial x} + \frac{\partial v}{\partial y}\right)$$

$$\tau_{xy} = \tau_{yx} = -\mu\left(\frac{\partial u}{\partial y} + \frac{\partial v}{\partial x}\right).$$

The various parameters and dependent variables ρ, u, v, μ, λ, E, k, T, and p are, respectively, the density, the x and y components of velocity, the shear and second coefficients of viscosity, the total energy per unit volume, the coefficient of heat conduction, the temperature, and pressure. An equation of state $p = p(e,\rho)$ relates the pressure to the density and the specific internal energy e,

$$e = (E/\rho) - \frac{1}{2}(u^2 + v^2). \tag{2.3}$$

For example, for ideal gases the equation of state is

$$p = (\gamma-1)\rho\left[e + \frac{1}{2}(u^2 + v^2)\right] \tag{2.4}$$

where γ is the ratio of specific heats at constant pressure and volume, respectively.

The numerical algorithm used in the next section is based on solving a set of difference equations which approximate the full Navier-Stokes equations (2.1) - (2.4). However, in considering the perturbation model we make several rather crude simplifications.

We assume, first of all, that near the outflow boundary the steady state is given by a constant pressure p_0, constant density ρ_0, a vanishing vertical velocity $v_0 = 0$, and that the velocity in the x-direction is given by

$$u_0 = \begin{cases} U_\infty & (\delta \leq y < \infty) \\ \alpha y & (0 \leq y \leq \delta) \end{cases} \tag{2.5}$$

where δ is the nominal edge of the boundary layer and $\alpha = \tau/\mu$ is the velocity gradient at the wall ($y = 0$). The shearing stress, τ, is, of course, a function of x but will not be treated as such in the development.

A second simplification is to assume (for the mean steady flow) that the total enthalpy, H_0, is constant, i.e.:

$$\frac{\gamma}{\gamma-1}\frac{p_0}{\rho_0} + \frac{1}{2}(u_0^2 + v_0^2) = H_0 = \text{const.} \tag{2.6}$$

Equation (2.6) is equivalent to the assumption that we are perturbing around a steady flow of Prandtl number unity.

The perturbed field quantities are defined as departures from the assumed steady state described above:

$$\begin{aligned} u' &= u - u_0 \\ p' &= p - p_0 \\ \rho' &= \rho - \rho_0 \\ v' &= v. \end{aligned} \tag{2.7}$$

Thus, p' is the pressure perturbation, etc. Next, we linearize the Navier-Stokes equations in the boundary layer region ($0 < y < \delta$) by substituting (2.7) into (2.1) and retaining only first-order quantities in the primed variables. The resulting set of equations may be written as follows:

$$\frac{\partial \rho'}{\partial t} + \alpha y \frac{\partial \rho'}{\partial x} + \rho_0\left(\frac{\partial u'}{\partial x} + \frac{\partial v'}{\partial y}\right) = 0, \qquad \text{(continuity)} \qquad (2.8)$$

$$\frac{\partial u'}{\partial t} + \alpha y \frac{\partial u'}{\partial x} + \alpha v' + \frac{1}{\rho_0}\frac{\partial p'}{\partial x} = \nu_0 \frac{\partial^2 u'}{\partial y^2}, \qquad \text{(x-momentum)} \qquad (2.9)$$

$$\frac{\partial v'}{\partial t} + \alpha y \frac{\partial v'}{\partial x} + \frac{1}{\rho_0}\frac{\partial p'}{\partial y} = \nu_0 \frac{\partial^2 v'}{\partial y^2}, \qquad \text{(y-momentum),} \qquad (2.10)$$

and instead of the linearized energy equation we have the linearized constant enthalpy relationship:

$$\frac{\gamma}{\gamma-1} p' = \frac{\gamma}{\gamma-1}\frac{p_0}{\rho_0}\rho' - \rho_0 u_0 u'. \qquad (2.11)$$

In the above equation ν_0 is the kinematic viscosity at steady state conditions. We have also used the thin layer approximation in (2.9) and (2.10). We emphasize again that the perturbation equations (2.8) - (2.11) are valid only for $0 < y < \delta$. Outside this viscous region we shall derive another set of equations which then will have to be matched to the above equations. First, however, we set the modal analysis. Because (2.11) provides an algebraic relationship between p' and ρ' and u', it is necessary to consider only a three-vector, (ρ', u', v') for which we set the modal ansatz:

$$\begin{pmatrix} \rho' \\ u' \\ v' \end{pmatrix} = e^{i(\psi t + bx)} \begin{pmatrix} F_1(y) \\ F_2(y) \\ F_3(y) \end{pmatrix}. \tag{2.12}$$

Next, we normalize and nondimensionalize the various quantities as follows:

$$\eta = \alpha y/U_\infty, \quad G_1 = F_1/\rho_\infty, \quad G_2 = F_2/U_\infty, \quad G_3 = F_3/U_\infty,$$

$$\omega = \psi/\alpha, \quad \beta = U_\infty b/\alpha, \quad \varepsilon = \alpha\nu_0/U_\infty^2 = 1/R_\delta,$$

where R_δ is the Reynolds number based on the boundary layer thickness.

In terms of the dimensionless variables and parameters, after substituting (2.12), equations (2.8) - (2.10) become, for $0 < \eta \leq 1$:

$$i(\omega + \beta\eta)G_1 + i\beta G_2 + G_3' = 0 \tag{2.13}$$

$$i(\omega + \frac{\beta}{\gamma}\eta)G_2 + \frac{i\beta}{\gamma M_\infty^2} G_1 + G_3 = \varepsilon G_2'' \tag{2.14}$$

$$i(\omega + \beta\eta)G_3 + \frac{1}{\gamma M_\infty^2} G_1' - \frac{\gamma-1}{\gamma}\eta G_2' - \frac{\gamma-1}{\gamma} G_2 = \varepsilon G_3''. \tag{2.15}$$

In equation (2.13) - (2.15) the primes designate differentiation with respect to the coordinate η; e.g., $G_3' = dG_3/d\eta$, $G_3'' = d^2 G_3/d\eta^2$.

Next, we consider the inviscid region, $\eta > 1$ where $u_0 = U_\infty$ and the flow is described well by the Euler equations ($\varepsilon = 0$). Repeating the above procedure the acoustic perturbation equations corresponding to (2.13) - (2.15) are derived:

$$i(\omega + \beta)G_1 + i\beta G_2 + G_3' = 0 \tag{2.16}$$

$$i(\omega + \frac{\beta}{\gamma})G_2 + \frac{i\beta}{\gamma M_\infty^2} G_1 = 0 \tag{2.17}$$

$$i(\omega + \beta)G_3 + \frac{1}{\gamma M_\infty^2} G_1' - \frac{\gamma-1}{\gamma} G_2' = 0. \tag{2.18}$$

The solvability conditions for the existence of solutions of the form $e^{r\eta}$ for the above homogeneous set of differential equations is found, after some manipulation, to be

$$r^2 = \beta^2 - \gamma M_\infty^2 (\omega + \frac{\beta}{\gamma})(\omega + \beta). \tag{2.19}$$

The set of equations (2.13) - (2.15) constitutes a fifth-order system and requires five boundary conditions. Two of them are supplied by the no-slip condition at the plate:

$$G_2(0) = 0 \tag{2.20}$$

$$G_3(0) = 0. \tag{2.21}$$

The other three are supplied by requiring the correct "impedance-matching" at $\eta = 1$ between the system (2.13) - (2.15) and the set (2.16) - (2.18), namely:

$$G_1'(1) = rG_1(1) \tag{2.22}$$

$$G_2'(1) = rG_2(1) \tag{2.23}$$

$$G_3'(1) = rG_3(1), \tag{2.24}$$

where $r = r(M_\infty; \omega,\beta)$ is given by (2.19).

The system (2.13) - (2.15) with the boundary conditions (2.20) - (2.24) constitutes the eigenvalue problem from which, in principle, we could extract the dispersion relation $\omega = \omega(\beta)$ for given Mach and Reynolds numbers (M_∞ and ε^{-1}).

As mentioned in the introductory section, we are interested in very long waves, i.e., the small β. We, therefore, propose expanding the eigenfunctions G_i $(i = 1,2,3)$ in the form

$$G_i = G_i^{(0)} + \beta G_i^{(1)} + \beta^2 G_i^{(2)} + \cdots \qquad (i = 1,2,3) \qquad (2.25)$$

where

$$G_i^{(0)} = \left[G_i(\eta;\omega,\beta,\varepsilon)\right]_{\beta=0}. \qquad (2.26)$$

We also expand the dimensionless "frequency" ω (which for small β will turn out to be the decay rate) in a similar manner:

$$\omega = \omega_0 + \beta\omega_1 + \cdots \qquad (2.27)$$

where

$$\omega_0 = [\omega]_{\beta=0}. \qquad (2.28)$$

Using the expansions (2.25) and (2.27) in (2.13) - (2.15), we get the following zeroth and first-order problems in β:

$$i\omega_0 G_1^{(0)} + G_3^{(0)\prime} = 0 \tag{2.29}$$

$$i\omega_0 G_2^{(0)} + G_3^{(0)} - \varepsilon G_2^{(0)\prime\prime} = 0 \tag{2.30}$$

$$i\omega_0 G_3^{(0)} + \frac{1}{\gamma M_\infty^2} G_1^{(0)\prime} - \frac{\gamma-1}{\gamma}\left(\eta G_2^{(0)}\right)' - \varepsilon G_3^{(0)\prime\prime} = 0 \tag{2.31}$$

and

$$i\omega_0 G_1^{(1)} + G_3^{(1)\prime} = -i\omega_1 G_1^{(0)} - iG_2^{(0)} - i\eta G_1^{(0)} \tag{2.32}$$

$$i\omega_0 G_2^{(1)} + G_3^{(1)} - \varepsilon G_2^{(1)\prime\prime} = -i\left(\omega_1 + \frac{\eta}{\gamma}\right)G_2^{(0)} - \frac{i}{\gamma M_\infty^2} G_1^{(0)} \tag{2.33}$$

$$i\omega_0 G_3^{(1)} + \frac{1}{\gamma M_\infty^2} G_1^{(1)} - \frac{\gamma-1}{\gamma}\left(\eta G_2^{(1)}\right)' - \varepsilon G_3^{(1)\prime\prime} = -i(\omega_1 + \eta)G_3^{(0)}. \tag{2.34}$$

Similar sets of equations can be derived for higher powers in β. They all have the same left-hand side in the relevant variables, with right-hand sides serving as source terms made up of all previous (presumably known) approximations. It is seen that ω_0, the zeroth-order approximation to the decay rate is determined from the "$\beta = 0$ problem," equations (2.29) - (2.31), without reference to $\omega_1 = (d\omega/d\beta)_{\beta=0}$, the phase velocity of the perturbations. We, therefore, first concentrate our attention on this "$\beta=0$ problem." By some simple manipulations one can extract from the system (2.29) - (2.31) a single fourth-order differential equation for $G_2^{(0)}$. For the sake of neater notation set $G_2^{(j)} = g_j$, $(j = 0,1,\cdots)$. With this change of notation, the fourth-order differential equation for $g_0 = G_2^{(0)}$ is found to be

$$\left(i\frac{\varepsilon}{\omega_0} - \frac{\gamma}{\gamma-1}\sigma\varepsilon^2\right)g_0^{IV} + \left(1 + i\frac{2\gamma}{\gamma-1}\sigma\varepsilon\omega_0\right)g_0'' - \sigma\eta g_0' - \sigma\left(1 - \frac{\gamma}{\gamma-1}\omega_0^2\right)g_0 = 0. \tag{2.35}$$

The boundary conditions for (2.35) are, to zeroth order in β:

$$g_0(0) = g_0''(0) = 0 \tag{2.36}$$

$$g_0'(1) = i\sigma^{1/2}\left(\frac{\gamma}{\gamma-1}\right)^{1/2}\omega_0\, g_0(1) \tag{2.37}$$

$$g_0'''(1) = i\sigma^{1/2}\left(\frac{\gamma}{\gamma-1}\right)^{1/2}\omega_0\, g_0''(1). \tag{2.38}$$

In equations (2.35) - (2.38), $\sigma = (\gamma-1)M_\infty^2$. For high Reynolds number flow, say $R_\delta > 30$, ε is a small number, and we can ask ourselves how does the eigenvalue ω_0 behave as a function of ε as ε diminishes and approaches zero.

There are three possibilities:

$$\lim_{\varepsilon\to 0}\frac{\varepsilon}{\omega_0} = \begin{cases} 0 \\ \infty \\ \text{constant} \end{cases}.$$

Another way to pose this is to say that $\omega_0 \sim \varepsilon^a$ as $\varepsilon \to 0$ and we ask whether a is smaller, greater than, or equal to zero. If $a < 0$, then we have in (2.35) a singular perturbation problem and one can show that, considering the boundary conditions (2.36) - (2.38), the only way to match the inner and outer expansions is to have the trivial solution. If $a > 0$, we have a regular

perturbation problem, and again the only possible solution is the trivial one of $g_0(\eta) \to 0$ as $\varepsilon \to 0$. We thus remain with the third possibility of $\omega_0 \sim \varepsilon$ for small ε. Let this proportionality constant be $\varepsilon/\omega_0 = \lambda_0$. Then (2.35) is rewritten as:

$$\left(i\lambda_0 - \frac{\gamma\sigma}{\gamma-1}\varepsilon^2\right)g_0^{IV} + \left(1 + i\,\frac{2\gamma}{\gamma-1}\,\sigma\,\frac{\varepsilon^2}{\lambda_0}\right)g_0'' - \sigma\eta g_0' - \sigma\left(1 - \frac{\gamma}{\gamma-1}\,\frac{\varepsilon^2}{\lambda_0^2}\right)g_0 = 0. \qquad (2.39)$$

It is assumed, and will be verified, that for reasonable Mach numbers, say below hypersonic speeds, $\lambda_0 = O(1)$.

We can now state the "$\beta = 0$ problem" more concisely: given σ, ε, and γ (i.e., the Mach number, Reynolds number, and the gas constant) solve the differential equation (2.39), subject to boundary conditions (2.36) - (2.38), for the eigenvalues λ_0 and the eigenfunction $g_0(\eta) = G_2^{(0)}$. This eigenvalue problem was solved numerically for a range of values $0 < \varepsilon \leq .05$, $0 < \sigma \leq 20$ (for laminar flow this corresponds roughly to Reynolds number, $50 \leq R_\infty < \infty$ and Mach number, $0 < M_\infty \lesssim 7$ for $\gamma = 1.4$). For this range of the parameters it is found that λ_0 is purely imaginary negative--this means that ω_0 is purely imaginary positive. Thus, ω_0 represents the decay rate of very long waves--to be corrected for finite but long waves by the term $\beta\omega_1$. Figure 1 shows a plot of $|1/\lambda_0|$ versus σ; for $0 < \varepsilon < .0053$ ($10^3 < R_\infty < \infty$), λ_0 is completely insensitive to changes in the Reynolds number and indeed may be taken to depend on the Mach number only. As $\sigma \to 0$, $|1/\lambda_0|$ takes on the value $\pi^2/4$ which can be derived analytically.

It is seen from Figure 1 that, for this range of parameters, $|\lambda_0|$ is indeed of order unity, $.4 \lesssim |\lambda_0| \lesssim 5$. For R_∞ as low as 40 (not shown on

the graph) the $|1/\lambda_0|$ curve deviates from the one shown by less than 5%. Thus, we conclude that for moderate and high Reynolds numbers the very long wave ($\beta \approx 0$) decay rate is basically a universal function of $\sigma = (\gamma-1)M_\infty^2$. The correction, $\beta\omega_1$, to the decay is found by considering the first-order problem, (2.32) - (2.34), with its attendant boundary conditions. Again, one can extract from this system a single fourth-order differential equation for $g_1 = G_2^{(1)}$. After some manipulations the g_1-problem may be stated as follows:

$$\left(i\lambda_0 - \frac{\gamma}{\gamma-1}\sigma\varepsilon^2\right)g_1^{IV} + \left(1 + i\,\frac{2\gamma}{\gamma-1}\,\sigma\,\frac{\varepsilon^2}{\lambda}\right)g_1'' - \sigma\eta g_1' - \sigma\left(1 - \frac{\gamma}{\gamma-1}\,\frac{\varepsilon^2}{\lambda_0^2}\right)g_1 = R \qquad (2.40)$$

where

$$R = \gamma M_\infty^2(\omega_1 R_1 + R_2), \qquad (2.41)$$

$$R_1 = \frac{i\varepsilon}{\gamma M_\infty^2 \omega_0^2}\, g_0^{IV} - 2i\varepsilon g_0'' - 2\,\omega_0\, g_0 \qquad (2.42)$$

$$R_2 = \frac{i\varepsilon}{\gamma M_\infty^2 \omega_0^2}\,(\eta g_0''')' - \frac{i(\gamma+1)}{\gamma}\,\varepsilon\eta g_0'' - \frac{2i\varepsilon}{\gamma}\, g_0' - \frac{\omega_0(\gamma+1)}{\gamma}\,\eta g_0. \qquad (2.43)$$

The boundary conditions, to first-order in β, are found to be

$$g_1(0) = g_1''(0) = 0 \qquad (2.44)$$

$$g_1'(1) - i\sigma^{1/2}\left(\frac{\gamma}{\gamma-1}\right)^{1/2}\omega_0\, g_1(1) = i\left(\frac{\gamma\sigma}{\gamma-1}\right)^{1/2}\left(\omega_1 + \frac{\gamma+1}{2\gamma}\right)g_0(1) \qquad (2.45)$$

$$g_1'''(1) - i\sigma^{1/2}\left(\frac{\gamma}{\gamma-1}\right)^{1/2}\omega_0\, g_1''(1) = i\left(\frac{\gamma\sigma}{\gamma-1}\right)^{1/2}\left(\omega_1 + \frac{\gamma+1}{2\gamma}\right)g_0''(1), \qquad (2.46)$$

where in (2.40) - (2.46) for given σ and ε we already know, albeit numerically, g_0 and ω_0. In deriving the boundary conditions (2.45), (2.46) one has to expand the expression (2.19) for r in powers of β. One then finds that the expansion is valid only for β/ω_0 small compared to unity. (Exactly how small cannot be answered at this point without finding the radius of convergence for our expansion.) In physical terms, for laminar flow where $\delta \sim \sqrt{x}$, this constraint means that our analysis is restricted to modes whose wavelength is longer than the computational domain on the plate.

A solvability condition for the g_1-problem is found by multiplying (2.40) by the left null vector of the left-hand side operator of (2.40). Symbolically, we may write

$$\omega_1 = - \frac{\langle f, R_2 \rangle}{\langle f, R_1 \rangle} \tag{2.47}$$

where f is the left null vector to the system, including the boundary conditions. Numerical evaluation of (2.47), for the same range of the Reynolds and Mach numbers mentioned before, leads to the result that ω_1 is almost a universal constant in the present problem, namely

$$\omega_1 = - .295 \pm .002. \tag{2.48}$$

Now that we have the decay rate ω_0 and the phase velocity ω_1 for long waves, we can derive outflow boundary conditions.

Consider, e.g., the pressure perturbation:

$$p' \sim e^{i(\psi t + bx)}\, G(\eta) \tag{2.49}$$

where G is a linear combination of G_1 and G_2. Since the numerical solution of the finite difference approximation to the Navier-Stokes equations is often done in terms of dimensionless temporal and spatial variables, we define dimensionless time and x coordinates by

$$\theta = \frac{U_\infty\, t}{L}\,; \qquad \xi = \frac{x}{L} \tag{2.50}$$

where the reference length L is the distance from the leading edge to the outflow. Using $\psi = \alpha\omega$, $b = \alpha\beta/U_\infty$, and (2.50), we can cast (2.49) in the form

$$p' \sim e^{i\frac{R_\infty\, C_f}{2}(\omega\theta + \beta\xi)}\, G(\eta) \tag{2.51}$$

where C_f is the skin-friction coefficient,

$$\frac{1}{2} C_f = \frac{\tau}{\rho_\infty\, U_\infty^2}\,. \tag{2.52}$$

Using the long-wave dispersion relation

$$\omega = \omega_0 + \beta\omega_1$$

and $p' = p - p_\infty$, we find that

$$\frac{\partial p}{\partial \theta} = - \frac{C_f^2 \, R_\infty}{4|\lambda_0|} (p - p_\infty) + \omega_1 \frac{\partial p}{\partial \xi} \, . \tag{2.53}$$

The quantity $|1/\lambda_0|$ is, of course, given to us by Figure 1. The skin friction coefficient could in principle be obtained from the actual computation at any time level. However, within our approximation one may give an estimate for C_f taken, for example, from boundary layer theory. Thus, for laminar flow and subsonic Mach numbers we may use the Blasius value of $C_f \tilde{=} 2/3\sqrt{R_\infty}$. More on this in the section describing the numerical work which tested the efficacy of the boundary condition (2.53).

We close this section by noting that the same methodology used here to derive outflow boundary conditions for the flat-plate problem can be used to extract boundary condition on the downstream side of other configurations such as the conditions in the wake of an airfoil, flow in a pipe, and so on. Also, other quantities have perturbations which satisfy (2.53), and one might try to apply the outflow condition to them as well. Another potential application is for unsteady flows where the dispersion relation for (2.13) - (2.15) would be carried out around some central wavenumber β_c rather than around $\beta = 0$.

3. NUMERICAL RESULTS

In this section we present some numerical results for the boundary condition described above. These results are preliminary; more complete results will be presented elsewhere. Using the non-dimensionalization described above and the Blasius expression for C_f, the boundary condition (2.53) can be written as

$$\frac{\partial p}{\partial \theta} = A(p - p_\infty) + B \frac{\partial p}{\partial \xi} \tag{3.1}$$

where

$$A = -\frac{1}{9|\lambda_0|} \; ; \; B = \omega_1 .$$

We implemented (3.1) in a Navier-Stokes program using a version of the MacCormack scheme that is second-order accurate in time and fourth-order accurate in space [7]. The numerical scheme was time consistent and did not use any acceleration technique such as a local time step.

For our numerical experiment we used an $M_\infty = 0.4$ boundary layer. The unit Reynolds number (per foot) was 3.0×10^5. The inflow was taken at 1.0 feet from the leading edge. We performed calculations using two different locations of the outflow boundary; x = 2.067 feet and 3.0 feet from the leading edge respectively. In both cases we used a grid of 31 points in the y direction (exponentially stretched). In the x direction we used 17 and 31 grid points respectively for a mesh size of .067 feet. The inflow and initial data were obtained from a computer program which solved the boundary layer equations. Convergence to steady state was assumed when the maximum over the grid of $|\frac{\partial p}{\partial \theta}|$ was less than 10^{-6}.

The boundary condition (3.1) was compared with the condition (1.1). Equation (3.1) has the property that the steady state pressure is not forced to be equal to p. Thus, there may be some discrepancies in the steady state solution. The numerical experiments were designed to assess the behavior of (3.1) with regards to:

a) Convergence rate

b) Robustness with respect to changes in the coefficients

c) Quality of the steady state.

We summarize our results below.

Convergence to steady state was significantly accelerated by the use of (3.1). The boundary condition (1.1) requires specification of a parameter α. The convergence rate is sensitive to the choice of α. In [5] an optimal α for a class of problems is presented. Because of the length of the computer runs, we were unable to determine the optimal α for the present problem. For the case of the outflow boundary at $x = 3.0$ feet from the leading edge a steady state was obtained using (3.1) in 30880 time steps. Using (1.1) and $\alpha = 1.45$ the steady state required 97020 time steps. Using $\alpha = .6$ which would be obtained from the formula in [6] based only on the free stream velocities and sound speed significantly degraded the convergence rate. For the case of the boundary at $x = 2.067$ feet from the leading edge, the use of (3.1) required 20960 time steps for convergence. The same run with $\alpha = 2.71$ required 52080 time steps.

Robustness of the boundary condition (3.1) was tested by modifying the coefficient A in (3.1). A complete study has not yet been made, but decreasing A by a factor of 2 (outflow boundary at 2.067 feet) increased the number of time steps required for convergence by 560 and made only small changes in the final steady state.

The quality of the steady state was assessed both by comparing solutions generated by the two boundary conditions and by comparing the solutions generated by the two positions of the outflow boundary. We first consider the

case of the outflow boundary at 3.0 feet. In this case the outflow pressure obtained from using (3.2) differed from p_∞ by less than .04%. In Table I we indicate the value of U and V (horizontal and vertical velocities non-dimensionalized by U_∞) for the steady states obtained from (3.1) and (1.1). The data are presented at different x locations indexed by the grid point. (The outflow was at grid point 31.) In all cases the velocities are shown for the first grid point away from the wall as this was where the maximum relative difference occurred. The relative differences decreased significantly for grid points away from the wall where the velocities increased in magnitude.

Using (1.1), we observed a slight oscillation in V near the outflow. This may be due to the fact that the outflow pressure is fixed at the free stream pressure while the flow appears to undergo a very small acceleration. For the boundary condition (3.1), V decreases rapidly close to the outflow. Thus, V near the outflow appears to be incorrect with both boundary conditions. Away from the outflow it is clear that V is the quantity that is most sensitive to the boundary condition although the differences are small and may also be affected by truncation error. The horizontal velocities are very close. At grid point 27 the two values of U differ by about 1.7%.

In Table II we list the values of U obtained from using (1.1) and (3.1) with the outflow boundary at 2.067 feet from the leading edge (grid point 17). These are compared with the values obtained when the outflow boundary was at 3.0 feet from the leading edge. We assume these values are accurate for the problem of the plate extending to infinity. Ideally, one would want the solution to be independent of the position of the outflow boundary. The values in these tables are the first grid point away from the wall where the relative differences are greatest.

It is apparent from Table II that the values for U are very insensitive to the position of the outflow boundary and to the choice of (1.1) or (3.1). The values obtained from (3.1) are slightly less accurate, but the differences are very small. At grid point 15 the relative error is only about 1.5%. These errors decrease for grid points away from the wall.

The results in Table III show that there are significant boundary errors in V for both boundary conditions; however, these values are very small compared to the free stream values. At grid point 13 the relative error in V is about 8.5% for (3.1) and about 10.9% for (1.1). It would require a more complicated problem to assess the meaning of these differences.

The boundary condition (3.1) has also been used to compute the steady flow field over a curved surface. A particular example is the flow over a curved hump with the curvature chosen so as to accelerate the flow from $M_\infty = .7$ to $M_\infty = 0.76$. The height of the hump was .04 feet and the curvature extended over a range of 1.2 ft. The surface then became flat and the computational domain extended a further 1.2 ft downstream. The unit Reynolds number was 3.0×10^5 while the boundary layer thickness at inflow was .0095 ft. The Reynolds number based on the boundary layer height at inflow was 896.00. Using (1.1), and several different values of α, convergence to the tolerance described above could not be obtained. Using (3.1) convergence in 52,760 iterations was obtained.

Finally, we point out that the methodology described above can be applied to schemes that are inconsistent in time. As one example, we can consider systems of the form

$$E \frac{\partial \overline{U}}{\partial t} + \frac{\partial \overline{F}}{\partial x} + \frac{\partial \overline{G}}{\partial y} = 0$$

where the flux functions $\overline{F}$ and $\overline{G}$ are the same as in (2.1) and $E(\overline{U})$ is a preconditioning matrix (see [9] for appropriate examples). The matrix $E(\overline{U})$ can be included in the linearization with only slight changes in the algebra. (Note that $\frac{\partial \overline{U}_0}{\partial t}$ is zero so that the only modification is that $\frac{\partial \overline{U}'}{\partial t}$ is replaced by $E(U_0) \frac{\partial \overline{U}'}{\partial t}$).

A simpler example is the use of a uniform grid in the viscous region and a different (larger) uniform grid in the inviscid region with the local time step appropriate for stability used in each region. It is easy to see that on the differential equation level this can be modelled by a matrix E which is I in the viscous region and of the form $\frac{1}{B} I$ where B is some large number depending on boundary layer thickness. This only affects the inviscid matching conditions ((2.22) - (2.24)). We have found that the parameters λ_0 and ω_1 are insensitive to B, if $B = O(\varepsilon^{-1})$.

4. CONCLUSION

We have introduced a methodology which enables us to derive an outflow boundary condition for a range of steady flows. Preliminary results indicate that the resulting boundary condition may be effective in accelerating the computation of steady subsonic flows with little loss of accuracy and no free parameters to be determined. The method is also applicable to incompressible and supersonic flows. Extensions to unsteady flows are also possible.

REFERENCES

[1] MacCormack, R. W., in Lecture Notes in Physics, Vol. 8, p. 151, Springer-Verlag, New York/Berlin, 1971.

[2] Olson, L. E., P. R. McGowan, and R. W. MacCormack, Numerical Solution of the Time-dependent Compressible Navier-Stokes Equations in Inlet Regions, NASA TM-X-62338, (March 1974).

[3] Shang, J. S. and W. L. Hankey, Jr., Numerical Solution of the Navier-Stokes Equations for Supersonic Turbulent Flow over a Compression Ramp, AIAA Paper 75-4 (1975).

[4] MacCormack, R. W. and B. S. Baldwin, A Numerical Method for Solving the Navier-Stokes Equations with Application to Shock-Boundary Layer Interaction, AIAA Paper 75-1 (1975).

[5] Rudy, D. and J. C. Strikwerda, A Non-Reflecting Boundary Condition for Subsonic Navier-Stokes Calculations, J. Comp. Phys., 36, (1980), 55-70.

[6] Rudy, D. and J. C. Strikwerda, Boundary Conditions for Subsonic Compressible Navier-Stokes Calculations, Computers and Fluids, 9 (1981), 327-338.

[7] Bayliss, A., P. Parikh, L. Maestrello, and E. Turkel, A Fourth-Order Scheme for the Unsteady Compressible Navier-Stokes Equations, AIAA Paper 85-1694 (1985).

[8] Harris, J. E. and D. K. Blanchard, Computer Program for Solving Laminar, Transitional or Turbulent Compressible Boundary Layer Equations for Two-Dimensional and Axisymmetric Flow, NASA TM 83207 (1985).

[9] Turkel, E., Algorithms for the Euler and Navier-Stokes Equations for Supercomputers, NASA CR 172543, Progress and Supercomputing in Computational Fluid Dynamics, E. M. Murman and S. S. Abarbanel, (eds.), Birkhauser Boston, Inc., 1985, pp. 155-172.

Table I. Non-dimensionalized U and V obtained from (1.1) and (3.1) (y = .00088 ft.)

x grid point	U/U_∞ (1.1)	U/U_∞ (3.1)	V/V_∞ (1.1)	$(V/u)_\infty$ (3.1)
11	.1234	.1234	$.331 \times 10^{-4}$	$.331 \times 10^{-4}$
15	.1144	.1144	$.263 \times 10^{-4}$	$.261 \times 10^{-4}$
19	.1071	.1072	$.218 \times 10^{-4}$	$.213 \times 10^{-4}$
23	.1009	.1014	$.194 \times 10^{-4}$	$.174 \times 10^{-4}$
27	.09526	.09680	$.201 \times 10^{-4}$	$.131 \times 10^{-4}$
31	.08978	.09429	$.231 \times 10^{-4}$	$.0821 \times 10^{-4}$

Table II. Non-dimensionalized U obtained from (1.1) and (3.1) with outflow boundary at x = 2.07 ft. compared with values obtained with outflow boundary 3 ft. from leading edge (y = .00088 ft).

x grid point	U/U_∞ (1.1)	U/U_∞ (3.1)	U/U_∞ outflow at 3 ft. from leading edge
5	.1420	.1421	.1421
7	.1348	.1350	.1349
9	.1286	.1289	.1287
11	.1232	.1238	.1234
13	.1184	.1195	.1186
15	.1139	.1161	.1144
17	.1106	.1143	.1106

Table III. **Non-dimensionalized V obtained from (1.1) and (3.1) with outflow boundary at x = 2.07 ft. compared with values obtained with outflow boundary 3 ft. from leading edge (y = .00088 ft).**

x grid point	V/V_∞ (1.1)	V/V_∞ (3.1)	V/V_∞ outflow at 3 ft. from leading edge
5	$.542 \times 10^{-4}$	$.538 \times 10^{-4}$	$.538 \times 10^{-4}$
7	$.448 \times 10^{-4}$	$.441 \times 10^{-4}$	$.443 \times 10^{-4}$
9	$.388 \times 10^{-4}$	$.374 \times 10^{-4}$	$.380 \times 10^{-4}$
11	$.347 \times 10^{-4}$	$.320 \times 10^{-4}$	$.331 \times 10^{-4}$
13	$.325 \times 10^{-4}$	$.268 \times 10^{-4}$	$.293 \times 10^{-4}$
15	$.312 \times 10^{-4}$	$.202 \times 10^{-4}$	$.263 \times 10^{-4}$
17	$.302 \times 10^{-4}$	$.165 \times 10^{-4}$	$.238 \times 10^{-4}$

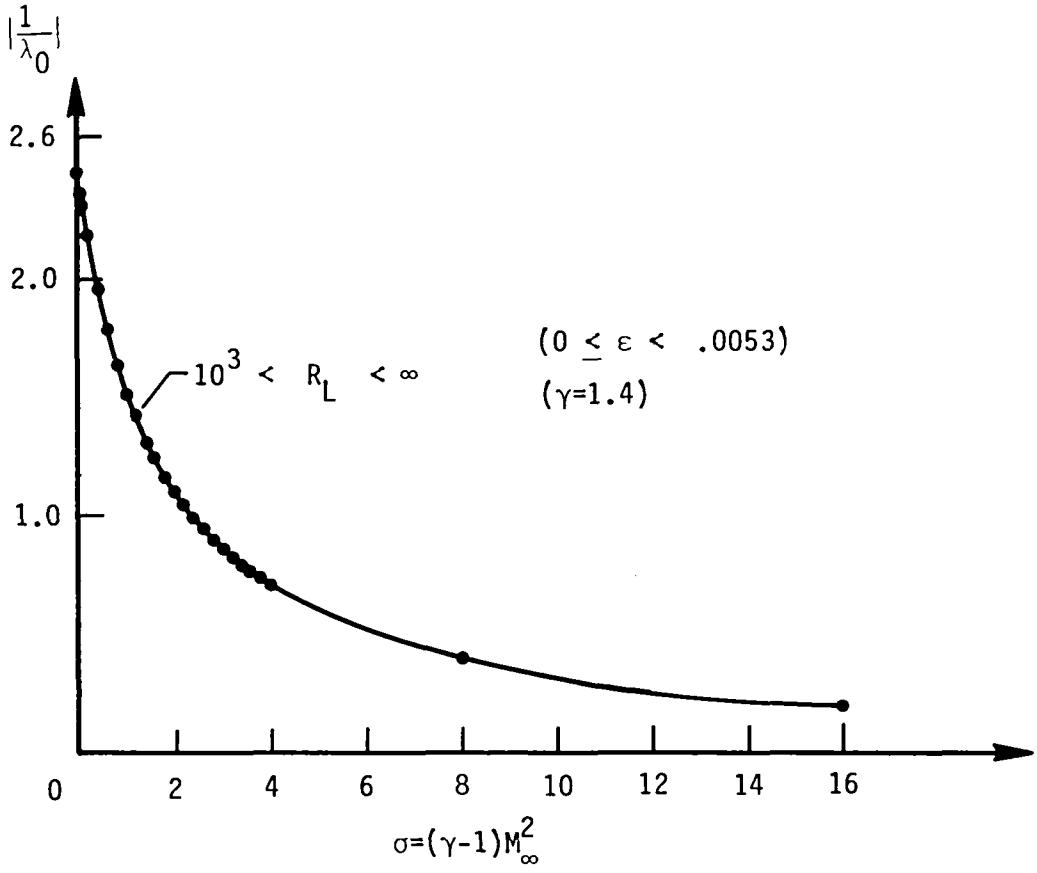

Figure 1.

1. Report No. NASA CR-178068 ICASE Report No. 86-9	2. Government Accession No.	3. Recipient's Catalog No.
4. Title and Subtitle NON-REFLECTING BOUNDARY CONDITIONS FOR THE COMPRESSIBLE NAVIER-STOKES EQUATIONS		5. Report Date March 1986 6. Performing Organization Code
7. Author(s) Saul Abarbanel, Alvin Bayliss, and Liviu Lustman		8. Performing Organization Report No. 86-9 10. Work Unit No.
9. Performing Organization Name and Address Institute for Computer Applications in Science and Engineering Mail Stop 132C, NASA Langley Research Center Hampton, VA 23665-5225		11. Contract or Grant No. NAS1-17070, NAS1-18107
12. Sponsoring Agency Name and Address National Aeronautics and Space Administration Washington, D.C. 20546		13. Type of Report and Period Covered Contractor Report 14. Sponsoring Agency Code 505-31-83-01

15. Supplementary Notes

Langley Technical Monitor:
J. C. South

Final Report

Invited Lecture, 7th Intl. Conf. on Computing Methods in Applied Science & Engineering, 12/9-13/85, Versailles, France (INRIA)

16. Abstract

A small perturbation analysis, in the long wavelength regime, is used to obtain the downstream boundary condition for the pressure for the flow over a flat plate. The methodology is extendable to other geometries. Numerical results for high Reynolds number laminar flows show great improvement in convergence rate to steady state as well as in the quality of the results.

17. Key Words (Suggested by Authors(s))	18. Distribution Statement
boundary conditions Navier-Stokes equations	34 - Fluid Mechanics & Heat Transfer 64 - Numerical Analysis Unclassified - unlimited

19. Security Classif.(of this report)	20. Security Classif.(of this page)	21. No. of Pages	22. Price
Unclassified	Unclassified	27	A03

For sale by the National Technical Information Service, Springfield, Virginia 22161

NASA-Langley, 1986

DO NOT REMOVE SLIP FROM MATERIAL

Delete your name from this slip when returning material to the library.

NAME	DATE	MS
[redacted]		

NASA Langley (Rev. Dec. 1991) RIAD N-75